

EFFECTS OF IFN ENTRAINMENT FROM ABOVE THE INVERSION ON ARCTIC BOUNDARY CLOUDS

William R. Cotton*, Gustavo Carrió and Hongli Jiang
Colorado State University, Ft. Collins, Colorado

1. INTRODUCTION

The Los Alamos National Laboratory CICE model (Hunke and Lipscomb 1999) was implemented into the real-time and research versions of the Colorado State University-Regional Atmospheric Modeling System (RAMS@CSU; Cotton et al. 2002). The original version of CICE was modified in its structure to allow module communication in an interactive multigrid framework. In addition, some improvements have been made in the routines involved in the coupling, among them, the inclusion of iterative methods that consider variable roughness lengths for snow covered ice thickness categories. The radiation scheme previously implemented in RAMS (Harrington 1997) was modified to take into account the cloud fraction provide an adequate coupling with the surface information generated by the sea-ice model. This version of the model also includes more complex microphysics that considers the nucleation of cloud droplets, allowing the prediction of mixing ratios and number concentrations for all condensed water species. The real-time version of RAMS@CSU automatically processes the NASA Team SSM/I F13 25km sea-ice coverage data; the data are objectively analyzed and mapped to the model grid configuration. We performed two types of cloud resolving simulations to assess the impact of the entrainment of aerosols from above the inversion on Arctic boundary layer clouds. The first group focuses on a well-documented mixed-phase cloud case while the second puts special emphasis on the evaluation of the potential effects of high IFN concentrations within upper layer on melting rates during spring-summer period.

2. DESIGN OF EXPERIMENTS

A mixed-phase cloud observed on May 4 1998 during the FIRE/SHEBA field experiment was chosen for a sensitivity study. Airborne IFN data for this Arctic boundary layer cloud were used to design the numerical experiments. The IFN vertical profile derived from the CSU CFD Ice Nucleus Counter data, exhibits relatively large concentrations above the boundary layer with a maximum value of $85.6 \ell^{-1}$, while below the inversion the vertical average is approximately $3 \ell^{-1}$. A brief description of the numerical experiments is given in following subsections. All the experiments have been performed in a two-dimensional (2-D) framework. The simulation domain is 5000m in the horizontal and approximately 3325 in the vertical. The vertical grid is stretched using the relationship $\Delta z_{k+1} = 1.05 \Delta z_k$ with 30 m spacing at the finest. Finally, both series of numerical experiments neglected non-inertial effects and used LANL CICE to provide surface properties and fluxes.

2.1 May 4 Case

The first set of experiments places special emphasis on studying how the structure of the cloud is affected by the entrainment of IFN from polluted air layer overriding the inversion. These set of 30 hour-long CRM simulations were initialized with the SHEBA sounding corresponding May 3 1998 23:00 UTC and different initial IFN based on the observed vertical profile. The control run assumed a constant "clean" profile for IFN ($3 \ell^{-1}$) within and above the boundary layer. All other simulations were initialized with clean IFN profile below the inversion, but with the observed IFN profile multiplied by factors between 1/3 and 2. A summary of the May 4 runs is given in Table 1.

*Corresponding author address: Prof. W.R. Cotton,
Colorado State Univ., Dept. of Atmospheric Science,
Ft. Collins, CO 80523-1371; FAX: 970-491-8449;
e-mail: cotton@atmos.colostate.edu

Table1

EXP	IFN
Control run	Clean
A.33	1/3 X observed
A.50	1/2 X observed
A1	1 X observed
A2	2 X observed

2.2 Multimonth CRM simulations

The second set of CRM simulation focused on the evaluation of the potential effects of high IFN concentrations within upper layer on melting rates during spring-summer period. The simulations were performed for the period May 1-July 31 using SHEBA soundings for initialization and nudging. The 4 May profile was used as a benchmark although the IFN concentration was assumed to be constant with altitude within the upper layer (at time=0). As done for the May 4 case, the initial IFN profile was assumed to be clean and polluted concentrations within and above the boundary layer, respectively. The concentrations assumed within each layer were also nudged considering the time-varying altitude of the inversion. Six ice thickness categories (with 4 internal layers) were considered to describe the sub grid scale ice thickness distribution and the linear remapping scheme of Lipscomb (2000) has been used to transfer ice among categories. The simulation conditions of CRM multi-month runs that correspond to results presented in this paper are summarized in Table 2.

Table2

Exp.	IFN (ℓ^{-1})
Control run	Clean
B.50	40
B1	80

3. RESULTS

3.1 May 4 Case

The time evolution of total condensate path (TCP) is shown in Figure 1a for A.33, A.50, A1, A2, and the control run. The total condensate path (TCP) increases when initial IFN concentrations above the inversion increases. On the other hand, the simulated liquid water paths also exhibit a monotonic behavior decreasing for higher initial IFN concentrations

within the upper layer (not shown). Figure 1b shows the percent decrease in the liquid water content (LWC) for experiment A1 with respect to the control run. The largest differences are linked to the IFN entrainment from above the inversion. Figures 1c and d show the differences in the long and short wave radiation reaching the surface simulated in runs A.33, A.50, A1 and A2 with respect to the control run. Longwave down differences are positive and mainly correlated with LWC differences. However, the lowest values correspond to the period in which the decrease in LWC is most important. Downward shortwave differences are negative and clearly correlated with the decrease in the liquid water content. Figure 2a shows the simulated profiles of the ice water content for 21:50Z, time at which IWC measurements were obtained from the CPI on the C-130 during FIRE.ACE and approximately the time at which the maximums of the simulated TCP are attained. The simulated IFN profiles are given in Figure 2b for the same time. It can be seen that horizontally averaged ice water contents exhibit a secondary maximum below the inversion that is consistent with the observations and could not be simulated unless a polluted upper layer was assumed for initialization.

3.2 Multimonth CRM simulations

Comparison between B.50 and B1 to the control run is presented in Figure 3. The differences in the simulated ice thickness, the liquid water fraction, and the net radiative forcing are given in Figures 3a, b, and c. In each case the ice thickness is calculated as a domain average of the areal means of sub-grid thickness distributions. The cloud liquid water fraction, evaluated as the ratio between the liquid water path and TCP of all vertical columns of the domain. It can be seen that increasing the IFN concentration above the inversion decreases liquid water fraction, increases net radiative forcing and therefore increases sea-ice melting rates.

4. CONCLUSIONS

Results indicate a significant impact of above boundary layer pollution on the microstructure of the simulated clouds. When assuming polluted initial profiles within the upper layer, the liquid water fraction of the cloud monotonically decreases, the total condensate

path increases, and downward IR tends to increase due to a significant increase in the ice water path.

Results corresponding to multi-month CRM simulations suggest that IFN entrainment from polluted air overriding the inversion may have a significant impact on sea-ice melting rates when mixed phase clouds are present. Similar experiments have been performed using observed cloud condensation nuclei (CCN) above the boundary layer for initialization. A preliminary analysis of the results indicates that the CCN effect on sea-ice melting rates is opposite though less important than the IFN effect.

Acknowledgements: This research was partially supported by the International Arctic Research Institute at the University of Alaska in Fairbanks under contract #UAF00-0086 and by the National Science Foundation under grant #ATM-0215367. Brenda Thompson is also acknowledged for her assistance in preparing this manuscript.

REFERENCES

- Cotton, W. R., R.A. Pielke, Sr., R.L. Walko, G.E. Liston, C.J. Tremback, H. Jiang, R. L. McAnelly, J. Y. Harrington, M.E. Nicholls, G.G. Carrio and J. P. McFadden 2002: RAMS 2001: Current Status and future directions. *Meteor. Atmos. Physics*, in press.
- Harrington, J. Y., 1997: The effects of radiative and microphysical processes on simulated warm and transition-season arctic stratus clouds. PhD Dissertation. Colorado State University, Fort Collins, CO, 287pp.
- Hunke, E. C., and Lipscomb, 1999: CICE: The Los Alamos sea-ice model, documentation and software, version 2.0, Los Alamos National Laboratory, LA-CC-98-16, v.2.
- Lipscomb, W. H., 2001: Remapping the Thickness Distribution of Sea Ice. *J. Geophys. Res.*, **106**, 13989-14000.

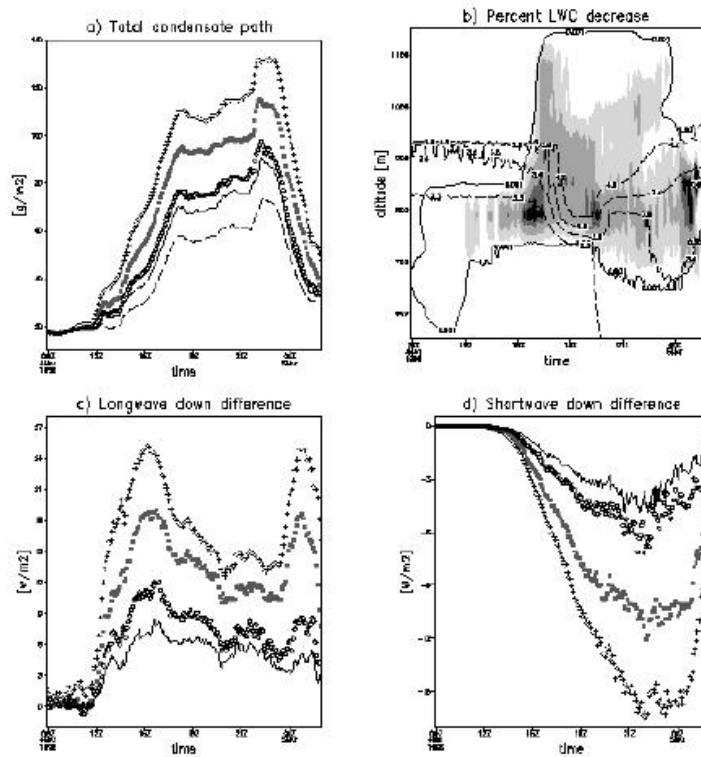


Figure 1. In panels a), c) and d), dashed lines, solid lines, open circles, closed squares and crosses denote control run and experiments A.33, A.50, A1 and A2, respectively. Shaded areas in panel (b) represent percent differences in LWC corresponding to A1 respect to control run. The increasing shading intensity from white indicates differences higher than 15, 30, 40, and 50 %. In this panel, the contours of horizontally averaged IFN concentrations (ℓ^{-1}) are denoted with dashed lines. The 0.001 gm^{-3} LWC contour has also been superimposed in panel (b) to indicate liquid cloud boundaries.

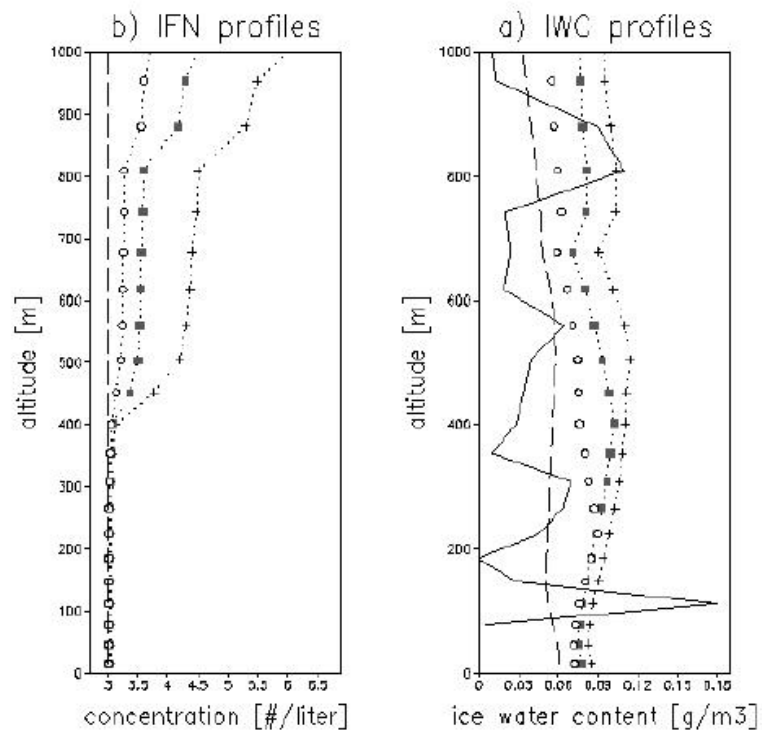


Figure 2. In panels (a) and (b) dashed lines, open circles, solid squares and crosses denote and denote control run and experiments A.50, A1 and A2, respectively. Solid line in panel (a) represents observed values of IWC.

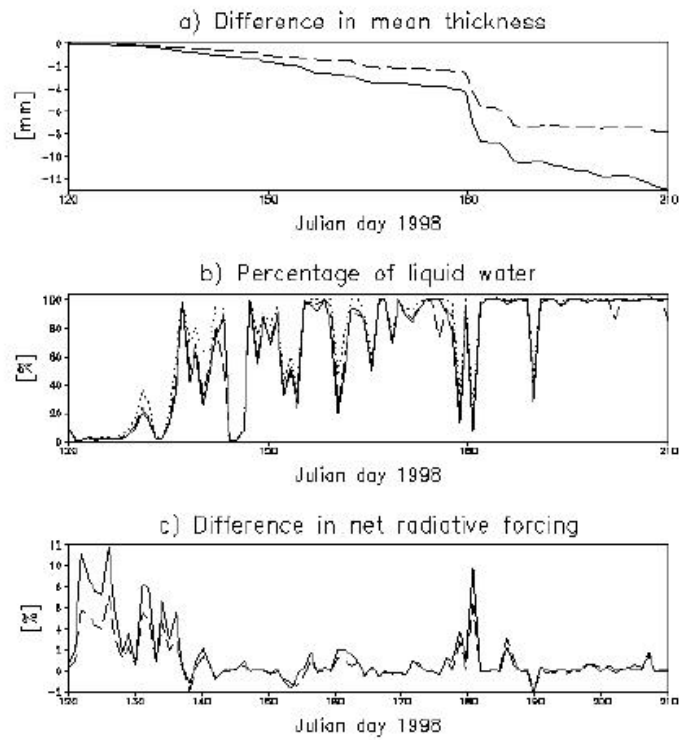


Figure 3. In panels (a) and (c) dashed and solid lines represent differences respect to the control run between corresponding to runs B.50 and B1, respectively. While in panel (b) dotted, dashed and solid lines denote control run, B.50 and B1, respectively.